

## MICROSTRUCTURAL ASPECTS OF CAST Fe-Cr-Mo-C ALLOY

WIECZERZAK Krzysztof<sup>1\*</sup>, BAŁA Piotr<sup>1,2</sup>, STĘPIEŃ Milena<sup>2</sup>, CIOŚ Grzegorz<sup>2</sup>, KOZIEŁ Tomasz<sup>1</sup>

<sup>1</sup> AGH University of Science and Technology, Faculty of Metals Engineering and Industrial Computer Science, Cracow, Poland, EU, [kwiecz@agh.edu.pl](mailto:kwiecz@agh.edu.pl)

<sup>2</sup> AGH University of Science and Technology, Academic Centre for Materials and Nanotechnology, Cracow, Poland, EU

### Abstract

Fe-25Cr-5Mo-0.82C alloy was synthesized in an arc furnace in high purity argon atmosphere and crystallized on water-cooled copper mould. The cross section of the ingot was examined by light microscopy, scanning electron microscopy (SEM), X-ray diffraction (XRD) and its Vickers hardness determined. The microstructure is composed of primary and secondary dendrites Fe-Cr-Mo solid solution with equiaxed and elongated morphology, depending on the nature of the crystallization. In the interdendritic regions complex  $M_{23}C_6$  carbides are present. The average hardness of the alloy is  $264 \pm 5$  HV10.

**Keywords:** Fe-Cr-Mo-C alloy, cast alloy, carbides, SEM, XRD

### 1. INTRODUCTION

In Fe-Cr-C alloys, produced with conventional techniques, it is possible to obtain microstructures composed of  $\alpha$ -ferrite and complex carbides such as  $M_3C$ ,  $M_7C_3$  and  $M_{23}C_6$  [1-3]. The formation of the various types of carbides depends on the chemical composition of the alloy [4, 5]. Alloys from Fe-Cr-C system are used as tool steels and hardfacing materials [6-10]. It should be mentioned that complex chromium carbides are also commonly used as a strengthening phase in nickel based superalloys and cobalt based alloys (Stellites), in many cases being present in association with the MC carbides ( $M = Nb, Zr, Ta, Hf$ ) [11-20].

Molybdenum in Fe-Mo-C alloys can form MoC,  $Mo_2C$  and complex-type carbides such as  $M_{23}C_6$  or  $M_6C$  [3, 21-23]. According to Palcut et al. [24] in low alloyed steels molybdenum stabilizes the MC carbide, reduces the molar fraction of  $M_7C_3$  carbide and decreases the values of Fe/Cr ratio in  $M_7C_3$  at lower temperatures. Inoue and Masumoto [3] described, inter alia, the tempering process and in-situ transformation of cementite to  $M_7C_3$ ,  $M_7C_3$  to  $M_{23}C_6$ , and  $M_{23}C_6$  to  $M_6C$ , which occur in Fe-3.6C-17.8Cr-xMo alloys ( $x = 3.6$  or  $8$ , wt.%). Transformation of cementite to  $M_7C_3$  starts approx.  $600^\circ C$  and it is completed at approx.  $700^\circ C$ . Further transformations occur at  $700^\circ C$ , requiring longer times of tempering.

It is known, that the wear resistance of tool and hardfacing alloys depends - on the volume fraction, type and morphology of carbides, and properties of the matrix as well [25-29].

In this study the analysis of the microstructure of the Fe-Cr-Mo-C ingot, produced in an arc furnace, is presented. Particular emphasis is placed on the determination of the morphology of eutectic, complex carbides.

### 2. EXPERIMENTAL

The Fe-Cr-Mo-C alloy was synthesized in an arc furnace Arc Melter AM (Edmund Bühler GmbH) in a Ti-gettered argon atmosphere. Melting of the charge was performed on a water-cooled copper mould. For further investigation the ingot, with a mass of approx. 35 g, was cut in half along the line A-A', as shown in **Fig. 1**.

The chemical composition was determined in the cross-section with optical emission spectrometer Foundry-Master (WAS). In order to estimate the segregation in the ingot a series of measurements on the bottom and on the cross section of the ingot were performed. Results are summarized in **Table 1**.

The X-Ray diffraction (XRD) analysis was performed by using a Panalytical Empyrean diffractometer using CoK $\alpha_1$  radiation ( $\lambda=1.7890$  Å).

The microstructure of the alloy was examined by Nikon LV150N light microscope and FEI VERSA 3D scanning electron microscope, equipped with the energy dispersive spectroscopy (EDS) detector. Microstructure investigations were carried out on the cross-section of the ingot, after polishing and etching. The microstructure of the samples was revealed by a solution of 30 g NH<sub>4</sub>F, 50ml HNO<sub>3</sub> and 20ml H<sub>2</sub>O.

Vickers hardness measurements were performed on a TUKON 2500 hardness tester.

### 3. RESULTS AND DISCUSSION

**Table 1** shows chemical composition of the ingot. That was found in the bottom and in the cross section of the ingot. As can be seen, the average carbon content varies significantly from 0.61 at the bottom to 0.82 (wt. %) for the cross section. It is also clear, that a segregation of molybdenum took place, as wt. % of Mo varies from 4.66 at the bottom to 5.33 for the cross section.

**Table 1** Chemical composition of the ingot (wt.%)

Place of measurements	C	Si	Mn	Cr	Mo	P	S	Fe
Cross-section	0.815	0.159	0.094	24.900	5.330	0.015	0.026	Bal.
Bottom	0.613	0.206	0.100	24.600	4.660	0.100	0.014	Bal.

**Fig. 1** shows a photograph of the ingot and **Fig. 2** the microstructure of the cross section along line A-A' (**Fig. 1**). During solidification on a water-cooled copper mould, three distinctive zones A, B and C were formed, indicated in **Fig. 2**. Dendrites in zone A, nucleated and grew in a very short time. First dendrites has an equiaxed shape (**Fig. 3c**). **Fig. 3b** shows microstructure of zone B (**Fig. 2**), dendrites which grew parallel and opposite to the heat exchange direction, have a columnar shape. **Fig. 3a** shows dendrites, typical for zone C (**Fig. 2**), formed at the end of solidification. These dendrites have similar, equiaxed shape, such as in zone A, because their latent heat is extracted radially through the undercooled melt.

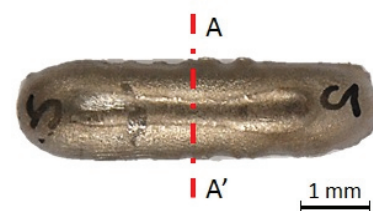


**Fig. 1** A Fe-Cr-Mo-C ingot with the cross section line A-A'

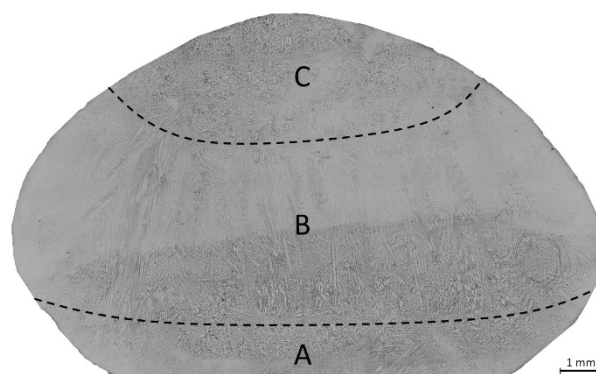


**Fig. 2** The reconstructed along A-A' cross-sectional microstructure of the ingot based on images from light microscope. A - refers to inner equiaxed zone, B - refers to columnar zone, and C - refers to outer equiaxed zone

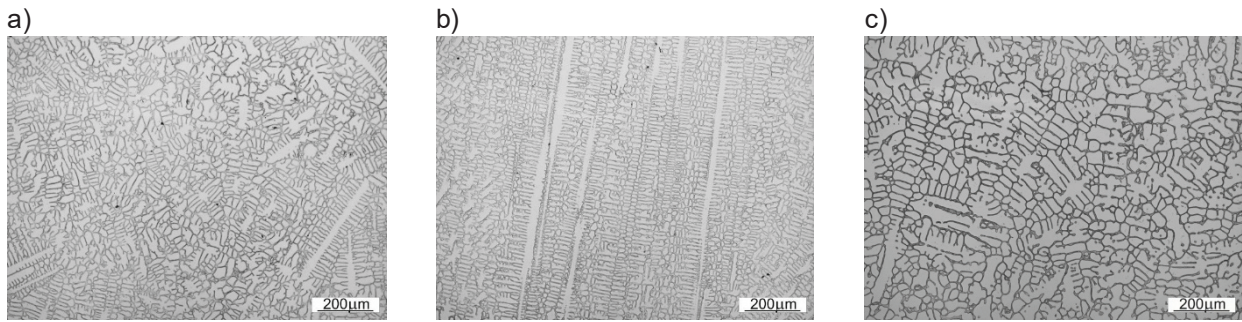


**Fig. 3** Microstructure of different zones along the transverse cross-section in Fe-Cr-Mo-C ingot: a - refers to outer equiaxed zone, b - refers to columnar zone, c - refers to inner equiaxed zone, light microscope

XRD patterns presented in **Fig. 4** show that the alloy consists of ferrite (Fe-Cr-Mo solid solution) and complex  $M_{23}C_6$  carbides.

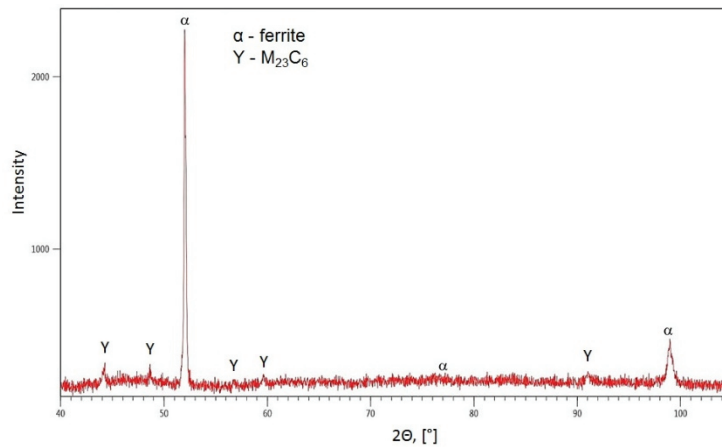
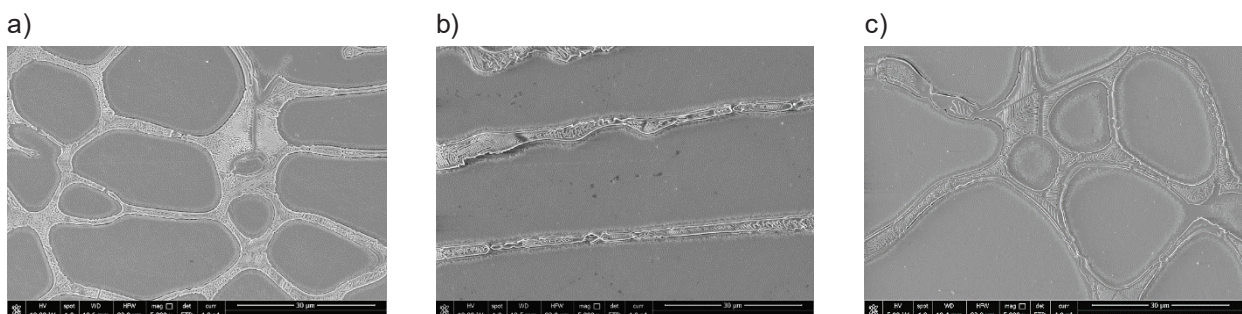


**Fig. 4** XRD patterns of the investigated alloy

**Fig. 5** shows the microstructure of eutectic  $M_{23}C_6$  carbides observed in the aforementioned three distinctive zones. It was observed that  $M_{23}C_6$  carbides formed in the interdendritic zones exhibit continuous, complex shapes. Carbides in outer and inner equiaxed zones have similar shapes. The boundary between eutectic carbides and matrix forms a continuous, longitudinal precipitation. Between the longitudinal boundaries, the carbides exhibit lamellar or polygonal character. In the columnar zone the eutectic has a longitudinal shape. Simultaneously lamellar precipitations within the eutectic boundaries make the whole a “ladder” shape.

**Fig. 6** shows the distribution of the major elements in dendrites and eutectic carbides. As seen, the eutectic zone is enriched in chromium and molybdenum, while the iron content is lowered.

The average hardness of the alloy is  $264 \pm 5$  HV10.



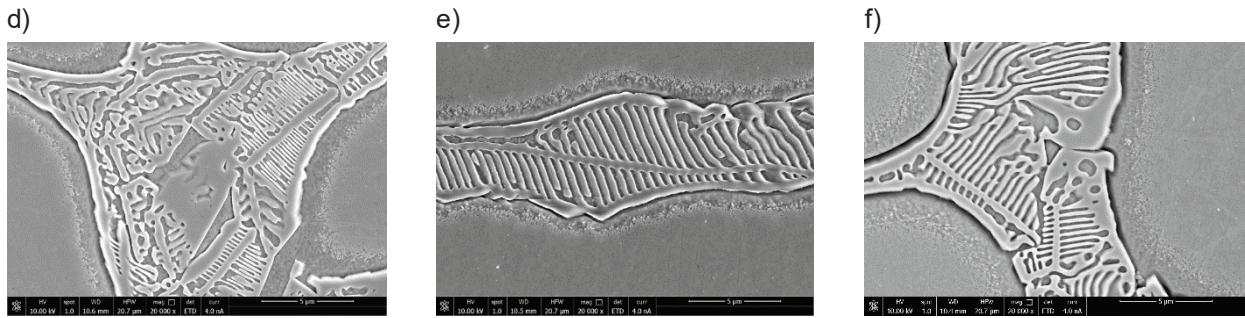


**Fig. 5** Microstructure of eutectic carbides in different zones along the transverse cross-section in Fe-Cr-Mo-C ingot: a,d - refers to outer equiaxed zone, b,e - refers to columnar zone, c,f - refers to inner equiaxed zone, SEM-SE

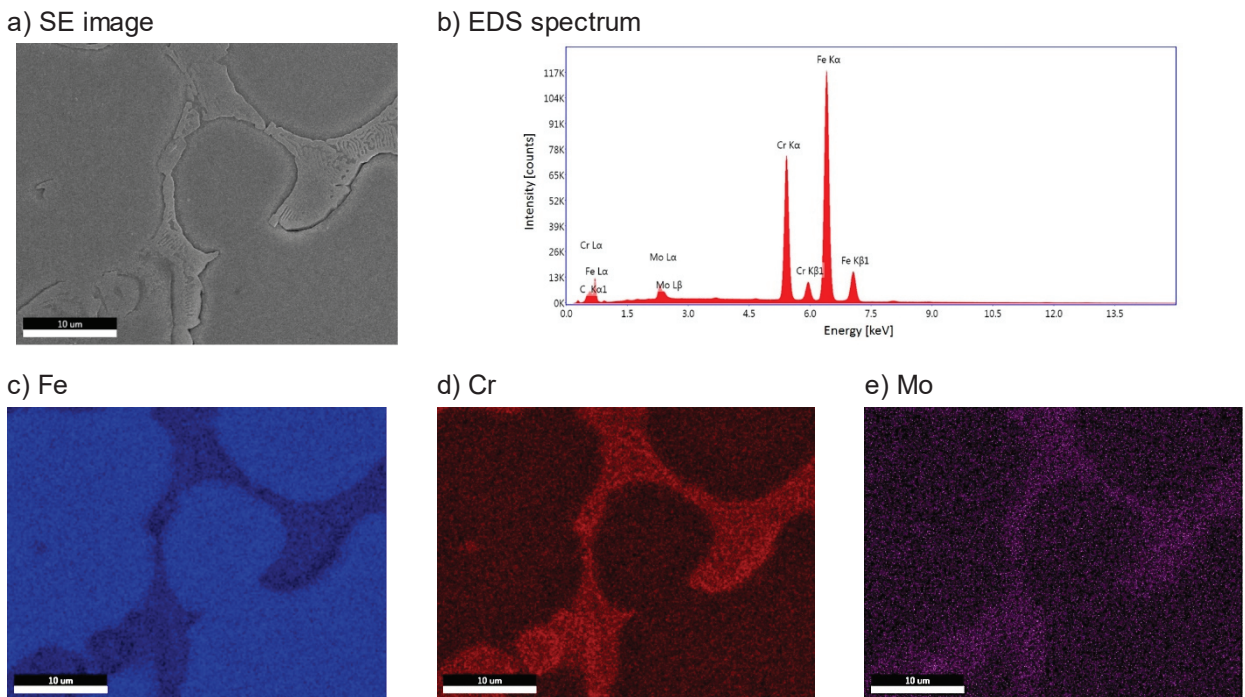


**Fig. 6** X-ray mapping of element distribution in dendrite and eutectic carbides

#### 4. CONCLUSION

Fe-Cr-Mo-C alloy was synthesized and characterized in the as cast state. It consists of ferrite (Fe-Cr-Mo solid solution) and complex  $M_{23}C_6$  carbides. The microstructure is composed of primary and secondary dendrites Fe-Cr-Mo solid solution with equiaxed and elongated morphology.  $M_{23}C_6$  carbides formed in the interdendritic zones exhibit continuous, complex shapes. The average hardness of the alloy is  $264 \pm 5$  HV10.

#### REFERENCES

- [1] ČEKADA M., PANJAN P., MAČEK M., ŠMÍD P. Comparison of Structural and Chemical Properties of Cr-based Hard Coatings, *Surface & Coatings Technology*, Vol. 152, 2002, pp. 31-35.
- [2] COLTTERS R.G., BELTON G.R. High Temperature Thermodynamic Properties of the Chromium Carbides  $Cr_7C_3$  and  $Cr_3C_2$  Determined Using a Galvanic Cell Technique, *Metallurgical Transactions A*, Vol. 14, 1983, pp. 1915-1919.

- [3] INOUE A., MASUMOTO T. Carbide Reactions ( $M_3C$ - $M_7C_3$ - $M_{23}C_6$ - $M_6C$ ) During Tempering of Rapidly Solidified High Carbon Cr-W and Cr-Mo Steels, *Metallurgical Transactions A*, Vol. 11, 1980, pp. 739-747.
- [4] VENKATRAMAN M., NEUMANN J.P. The C-Cr (Carbon-Chromium) System, *Bulletin Alloy Phase Diagrams*, Vol. 11, 1990, pp. 152-159.
- [5] KUO K. Carbide Precipitation in Tungsten-Chromium Steel Below 700°C, *Journal of the Iron and Steel Institute*, Vol. 185, 1957, pp. 297-303.
- [6] DOĞAN Ö.N., HAWK J. A., LAIRD G. Solidification Structure and Abrasion Resistance of High Chromium White Irons, *Metallurgical and Materials Transactions A*, Vol. 28, 1997, pp. 1315-1328.
- [7] FAN C., CHEN M.C., CHANG C.M., WU W. Microstructure Change Caused by  $(Cr,Fe)_{23}C_6$  Carbides in High Chromium Fe-Cr-C Hardfacing Alloys, *Surface & Coatings Technology*, Vol. 201, 2006, pp. 908-912.
- [8] CHANG C.M., CHEN Y.C., WU W. Microstructural and Abrasive Characteristics of High Carbon Fe-Cr-C Hardfacing Alloy, *Tribology International*, Vol. 43, 2010, pp. 929-934.
- [9] BYELIKOV S., VOLCHOK I., NETREBKO V. Manganese Influence on Chromium Distribution in High-Chromium Cast Irons, *Archives of Metallurgy and Materials*, Vol. 58, 2013, pp. 6-8.
- [10] SOHAR C.R., BETZWAR-KOTAS A., GIERL C., WEISS B., DANNINGER H. Gigacycle Fatigue Behavior of a High Chromium Alloyed Cold Work Tool Steel, *International Journal of Fatigue*, Vol. 30, 2008, pp. 1137-1149.
- [11] BERTHOD P. High Temperature Properties of Several Chromium-Containing Co-based Alloys Reinforced by Different Types of MC Carbides (M = Ta, Nb, Hf and/or Zr), *Journal of Alloys and Compounds*, Vol. 481, 2009, pp. 746-754.
- [12] BERTHOD P., ARANDA L., VÉBERT C., MICHON S. Experimental and Thermodynamic Study of The High Temperature Microstructure of Tantalum Containing Nickel-based Alloys, *Calphad-Computer Coupling of Phase Diagrams and Thermochemistry*, Vol. 28, 2004, pp. 159-166.
- [13] BERTHOD P., HAMINI Y., ARANDA L., HÉRICHER L. Experimental and Thermodynamic Study of Tantalum-Containing Iron-Based Alloys Reinforced by Carbides: Part I - Case of (Fe,Cr)-based Ferritic Steels, *Calphad-Computer Coupling of Phase Diagrams and Thermochemistry*, Vol. 31, 2007, pp. 351-360.
- [14] BERTHOD P. High Temperature Oxidation Behavior of Chromium-Rich Alloys Containing High Carbides Fractions. Part I: Nickel-base Alloys, *Materials and Corrosion*, Vol. 64, 2013, pp. 567-577.
- [15] BAŁA P., PACYNA J. The Influence of Pre-Tempering on the Mechanical Properties of HS6-5-2 High Speed Steel, *Archives of Metallurgy and Materials*, Vol. 53, 2008, pp. 795-801.
- [16] BAŁA P. Microstructural Characterization of the New Tool Ni-Based Alloy with High Carbon and Chromium Content, *Archives of Metallurgy and Materials*, Vol. 55, 2010, pp. 1053-1059.
- [17] BAŁA P. Microstructure Characterization of High Carbon Alloy from the Ni-Ta-Al-Co-Cr System, *Archives of Metallurgy and Materials*, Vol. 57, 2012, pp. 937-941.
- [18] BAŁA P. High Carbon Alloys from the Ni-Ta-Al-M System, AGH University of Science and Technology Press, Krakow, 2012.
- [19] BAŁA P. The Dilatometric Analysis of the High Carbon Alloys from Ni-Ta-Al-M System, *Archives of Metallurgy and Materials*, Vol. 59, 2014, pp. 977-980.
- [20] CIOS G., BAŁA P., STĘPIEŃ M., GÓRECKI K. Microstructure of Cast Ni-Cr-Al-C, *Archives of Metallurgy and Materials*, Vol. 60, 2015, pp. 145-148.
- [21] GOLDSCHMIDT H.J. *Interstitial Alloys*, Springer Science+Business Media, LLC, New York, 1967.
- [22] MALKIEWICZ T. *Physical Metallurgy of Iron Alloys*, Publishing House PWN, Warsaw - Cracow, 1978 (in Polish).
- [23] LEE H.M., ALLEN S.M., GRUJICIC M. Coarsening Resistance of  $M_2C$  Carbides in Secondary Hardening Steels: Part II. Alloy Design Aided by a Thermochemical Database, *Metallurgical Transactions A*, Vol. 22, 1991, pp. 2869-2876.
- [24] PALCUT M., VACH M., CICKA R., JANOVEC J. Compositional Changes in Carbide  $M_7C_3$  Upon Annealing, *Archives of Metallurgy and Materials*, Vol. 53, 2008, pp. 1157-1164.

- [25] CHOTĚBORSKÝ R., HRABĚ P., MÜLLER M., SAVKOVÁ J., JIRKA M. Abrasive Wear of High Chromium Fe-Cr-C Hardfacing Alloys, Journal of Agricultural Engineering Research, Vol. 54, 2008, pp. 192-198.
- [26] CHOTĚBORSKÝ R., HRABĚ P., MÜLLER M., SAVKOVÁ J., JIRKA M., NAVRÁTILOVÁ M. Effect of abrasive particle size on abrasive wear of hardfacing alloys, Journal of Agricultural Engineering Research, Vol. 55, 2009, pp. 101-113.
- [27] MATTHEWS A., LEYLAND A., HOLMBERG K., RONKAINEN H. Design Aspects for Advanced Tribological Surface Coatings, Surface & Coatings Technology, Vol. 100-101, 1998, pp. 1-6.
- [28] DZIURKA R., MADEJ M., KOPYŚCIAŃSKI M., MALYSZKO M., DZIADOSZ M. The Influence of Microstructure of Medium Carbon Heat-Treatable Steel on Its Tribological Properties, Key Engineering Materials, Vol. 641, 2015, pp. 132-135.
- [29] ŁĘTKOWSKA B., DZIURKA R., BAŁA P. The Analysis of Phase Transformation of Undercooled Austenite and Selected Mechanical Properties of Low-Alloy Steel with Boron Addition, Archives of Civil and Mechanical Engineering, Vol. 15, 2015, pp. 308-316.